

Article

Genomic Identification of Callose Synthase (*CalS*) Gene Family in Sorghum (*Sorghum bicolor*) and Comparative In Silico Expression Analysis under Aphid (*Melanaphis sacchari*) Infestation

Kunliang Zou ^{1,2}, Yang Liu ³, Tonghan Wang ¹ , Minghui Guan ^{2,3}, Xiaofei Li ¹, Jieqin Li ^{1,2}, Haibing Yu ¹, Degong Wu ^{1,*}  and Junli Du ^{1,2,*}

¹ College of Agriculture, Anhui Science and Technology University, Chuzhou 233100, China; wlhjq@163.com (J.L.); yuhb@ahstu.edu.cn (H.Y.)

² Anhui Province International Joint Research Center of Forage Bio-Breeding, Chuzhou 233100, China

³ College of Resources and Environment, Anhui Science and Technology University, Chuzhou 233100, China

* Correspondence: wudg@ahstu.edu.cn (D.W.); adu83419@163.com (J.D.)

Abstract: Callose is widely present in higher plants and plays a significant role in plant growth, development, and response to various stresses. Although numerous studies have highlighted the importance of the callose synthase (*CalS*) genes, their role in the resistance of sorghum (*Sorghum bicolor*) to aphids (*Melanaphis sacchari*) remains limitedly understood. This study identified 11 sorghum callose synthase genes (*SbCalS*), unevenly distributed across four chromosomes of sorghum. All *SbCalS* proteins contain glucan synthase and Fks1 domains, with segmental duplication playing a major role in gene diversification. Cis-element prediction revealed the presence of numerous stress-responsive elements, indicating that this gene family is primarily involved in stress resistance. Using published RNA-seq data, we discovered the differential expression of the *SbCalS5* gene between resistant and susceptible sorghum varieties. Real-time quantitative PCR (qPCR) analysis confirmed the relative expression levels of all *SbCalS* members under aphid stress. To further verify the role of callose in sorghum, we measured the callose content in both resistant and susceptible sorghum varieties. The results indicated that callose plays a critical role in aphid resistance in sorghum, particularly the *SbCalS5* gene. This study provides a reference for further investigation into the role of callose synthase genes in sorghum aphid resistance.

Keywords: sorghum (*Sorghum bicolor*); expression analysis; callose; aphid (*Melanaphis sacchari*); callose synthase gene family



Citation: Zou, K.; Liu, Y.; Wang, T.; Guan, M.; Li, X.; Li, J.; Yu, H.; Wu, D.; Du, J. Genomic Identification of Callose Synthase (*CalS*) Gene Family in Sorghum (*Sorghum bicolor*) and Comparative In Silico Expression Analysis under Aphid (*Melanaphis sacchari*) Infestation. *Agronomy* **2024**, *14*, 1393. <https://doi.org/10.3390/agronomy14071393>

Academic Editors: Ivo Toševski, Iwona Sadura and Maciej Grzesiak

Received: 12 May 2024
Revised: 22 June 2024
Accepted: 25 June 2024
Published: 27 June 2024



Copyright: © 2024 by the authors. Licensee MDPI, Basel, Switzerland. This article is an open access article distributed under the terms and conditions of the Creative Commons Attribution (CC BY) license (<https://creativecommons.org/licenses/by/4.0/>).

1. Introduction

Sorghum, a C4 monocotyledonous herbaceous plant from the Poaceae family, is known for its high photosynthetic efficiency and robust resilience. As the fifth largest cereal crop globally [1], sorghum is widely cultivated and holds significant importance, especially in developing countries and semi-arid regions where resources are limited. In these areas, sorghum is primarily used for human consumption. Conversely, in developed countries, sorghum is mainly utilized for animal feed, industrial applications, and energy production [2–5].

Recently, sorghum aphids have become a major pest for sorghum plants, with their presence spreading across Asia, Africa, and the Americas. These aphids pose a serious threat to sorghum cultivation worldwide [6]. Their piercing-sucking feeding behavior leads to leaf wilting and dehydration, which directly affects the yield and quality of sorghum crops [7]. By feeding on the phloem tissue, aphids can cause plant tissues and leaves to desiccate, discolor, and necrotize. This damage can delay seedling development, inhibit tassel emergence, and cause grain heads to become sterile, with severe infestations

potentially resulting in plant death [8]. Aphid-induced stress can cause significant losses in grain yield and overall biomass. Additionally, the sticky honeydew secreted by aphids can promote the growth of sooty molds on leaf surfaces, further reducing the plants' photosynthetic capacity and exacerbating the damage [9].

In plants, the enzyme callose synthase, situated on the cell membrane, is responsible for callose production [10]. This enzyme is responsible for producing β -1,3-glucan, a key component in various physiological processes, including sieve tube metabolism and gametophyte development. These glucans are vital for spore formation, stomatal closure, and responses to biotic and abiotic stresses. The synthesis and degradation of callose are integral to plant growth, development, and metabolic processes [11]. Callose plays a significant role in sporogenesis, stomatal closure, and protection against various stresses. The production and breakdown of callose directly affect plant growth and metabolism. Research has identified synergistic interactions that enhance resistance to pathogens through callose involvement. For example, in *Arabidopsis thaliana*, PDLP1 protein enhances plant defense by regulating callose deposition around haustoria—specialized structures formed by downy mildew pathogens (*Hyaloperonospora arabidopsidis*) and fungi during host cell infection. This regulation aids in strengthening the plant's defense mechanisms against these pathogens [12]. The transient expression of the *PMR4* gene in *Arabidopsis thaliana*, which controls callose synthase, has been demonstrated to enhance osmotic resistance to barley powdery mildew [13]. Mycorrhiza induction in Tomato (*Solanum lycopersicum* L.) plants infected with *Staphylococcus aureus* results in upregulation of callose expression, confirming its relevance in plant defense [14]. When plants are attacked by hemipteran insects, they activate callose deposition, which obstructs the flow in the phloem. This obstruction reduces the amount of sap that the insects can extract from the phloem, thereby limiting their feeding [15]. In *Arabidopsis thaliana*, the *CALS1* gene, which encodes callose synthase, is upregulated following Tobacco whitefly (*Bemisia tabaci*) infestation, resulting in elevated callose accumulation [16]. An abundant accumulation of callose deposits was observed in wheat leaves infected with Russian wheat aphids (*Diuraphis noxia*) in sieve plates, companion cell plasmodesmata, and stylet tracks [17]. Recent research indicates that β -aminobutyric acid (BABA) enhances the expression of callose synthase genes in soybean seedlings, leading to accelerated callose deposition and significant inhibition of soybean aphid growth [18]. In cotton plants, the callose synthase gene *GhCalS5* plays a crucial role in regulating callose synthesis in leaves, thereby enhancing cotton resistance to aphids [19]. Variation in callose content upon infestation of watermelon (*Citrullus lanatus*) mesophyll cells by aphids is one of the distinguishing factors in watermelon resistance against cotton aphids (*Aphis gossypii* Glover) [20].

Research on callose deposition has been a hotspot in recent years. When higher plants are subjected to mechanical damage, bacterial invasion, insect infestation, or high temperatures, they promptly regulate callose synthesis in sieve tubes. Callose deposits on the sieve tube surface or within sieve pores prevent abnormal substance transport, thereby maintaining normal transport functions. Once the external stimuli are removed, deposited callose rapidly degrades, restoring the sieve tube's normal transport function [21,22]. When aphids pierce plants with their stylets, the plants perceive mechanical damage and salivary elicitors, activating a complex signaling network involving various plant hormones. These hormones regulate callose deposition through synergistic and antagonistic actions. For example, jasmonic acid (JA) and salicylic acid (SA) are crucial in enhancing callose deposition. Studies have shown that the SA and JA signaling pathways can trigger activation of the flg22 protein, leading to an oxidative burst and callose deposition [23]. *CalS* is key to callose production. Specific genes such as *GSL5* and *GSL7* are upregulated during biotic stress, resulting in increased callose synthesis and its deposition in sieve plates and plasmodesmata, thereby hindering aphid feeding [24,25]. Calcium signaling also plays a critical role in regulating callose deposition. Pathogen invasion triggers a rapid influx of Ca^{2+} ions into the cytoplasm, thereby activating calcium-dependent protein kinases (CDPKs). These kinases phosphorylate target proteins involved in the callose

synthesis pathway, thereby enhancing callose deposition [26]. Reactive oxygen species (ROS) serve as signaling molecules and directly act as antimicrobial agents, regulating callose deposition [27]. Moreover, ROS can influence the expression of defense-related genes, boosting the plant's defense mechanisms. Recent research highlights the importance of secondary metabolites and signaling peptides in controlling callose deposition. For example, the induction of glucosinolates and their degradation products has been shown to enhance callose deposition in response to aphid feeding [28]. Furthermore, signaling peptides derived from precursor proteins, such as the elicitor peptide 1 (Pep1), can amplify defense responses and promote callose deposition when the plant is damaged [29]. In summary, the regulation of callose deposition in response to aphid feeding is a multifaceted process involving complex signaling networks. These networks integrate hormonal signals, calcium signaling, ROS production and various secondary metabolites to coordinate a robust defense response. Interestingly, heavy metals like Al^{3+} and Cd^{2+} also play a role in regulating callose deposition in plants [30]. In (Figure 1), we present an overview of the latest insights into the function and regulation of callose biosynthesis in plants.

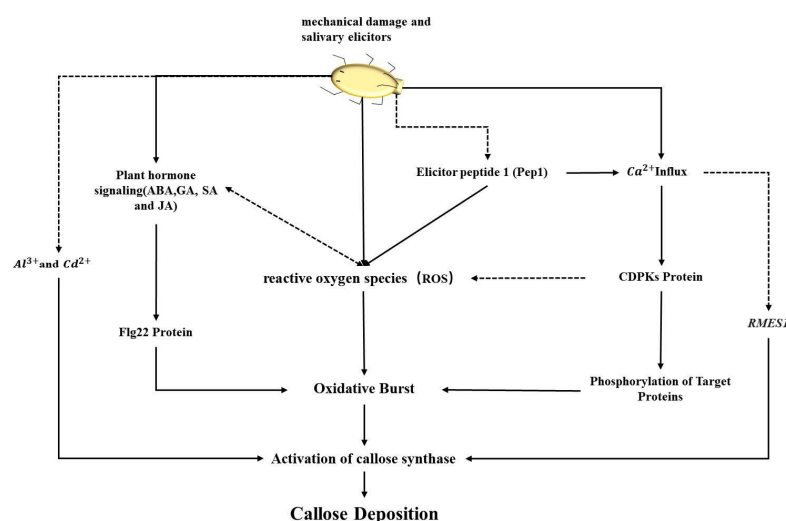


Figure 1. Regulatory pathways of callose deposition in plants infected by aphids. Solid lines indicate confirmed regulatory pathways, dashed lines indicate possible regulatory pathways, and bidirectional arrows indicate reciprocal regulation.

Based on this, we investigated the *SbCalS* genes, identifying 11 in the sorghum genome. We analyzed their phylogenetic relationships, gene structures, conserved motifs, and expression patterns. Additionally, we performed qPCR analysis of *SbCalS* gene expression in sorghum under aphid infestation. This study offers valuable insights into the role of callose in plant defense against insect pests.

2. Materials and Methods

2.1. Experimental Materials and Aphid Rearing

In this study, the plants used were two sorghum varieties with extreme aphid resistance identified from the sorghum germplasm repository at Anhui Science and Technology University: the resistant variety HX133 and the susceptible variety HX141. The identification method was based on Tetreault H M et al. [31]. All experiments included three biological replicates. Aphids were sourced from the common sorghum variety 'Tiegankangsi' and transferred to fresh sorghum plants biweekly to sustain their population. The plants were cultivated in an artificial climate chamber with a 16 h light/8 h dark photoperiod at 28 °C and 50–60% relative humidity. Regular watering and fertilization were maintained. All setups had three biological replicates.

2.2. Identification of the *SbCalS* Gene Family

In this study, we downloaded 12 *Arabidopsis thaliana* *CalS* genes [32] from the Ensembl Plants database (<https://plants.ensembl.org/index.html>, accessed on 22 February 2024) to use as reference sequences [33]. These sequences were then subjected to BLAST searches against the sorghum genome (*Sorghum bicolor*_NCBIv3) to identify candidate sorghum callose synthase (*SbCalS*) genes and their corresponding proteins. Subsequently, redundant sequences were removed, and the inferred sorghum *CalS* genes were examined using the Pfam (<http://pfam-legacy.xfam.org/>, accessed on 23 February 2024) [34] and NCBI Conserved Domain Database (CDD) programs to verify the presence of the *CalS* domain [35]. We excluded sequences lacking the conserved *CalS* enzyme domain and aligned the selected *CalS* domain amino acid sequences from sorghum using GeneDoc software (version 2.7) [36]. Finally, all predicted *SbCalS* protein sequences were analyzed using the SMART database (<https://smart.embl.de/>, accessed on 23 February 2024). The complete sequences of the β -1,3-glucan synthase domain (PF02364) were used to confirm the presence of true *CalS* in sorghum [37].

2.3. Physicochemical Characterization and Subcellular Localization Prediction of *SbCalS* Gene Family

We performed a predictive analysis of the physicochemical properties of *SbCalS* protein using the online software ProtParam provided by ExPaSy (<https://web.expasy.org/protparam/> accessed on 25 February 2024). Subsequently, we utilized the online tool WoLF PSORT (<https://wolfpsort.hgc.jp/>, accessed on 25 February 2024) to determine its subcellular localization [38]. We utilized SOPMA (https://npsa-prabi.ibcp.fr/cgi-bin/npsa_automat.pl?page=npsa%20_sopma.html, accessed on 26 February 2024) for predicting the secondary structure of the protein [39], while signal peptide prediction analysis was carried out using SignalP 4.0 Server (<https://services.healthtech.dtu.dk/>, accessed on 26 February 2024) [40]. Additionally, we used the DeepTMHMM server (<https://dtu.biolib.com/DeepTMHMM>, accessed on 26 February 2024) to predict the membrane topology and estimate the number of transmembrane helices in the complete protein dataset [41].

2.4. Prediction of Gene Structure and Cis-Acting Elements in the *SbCalS* Gene Family

Predicting conserved domains of *SbCalS* was done using MEME software (version 5.5.5) (<https://meme-suite.org/meme/>, accessed on 5 March 2024), with a total of 12 motifs selected while maintaining default parameters [42]. Extracting gene structure information from the sorghum GFF annotation file for *SbCalS* was accomplished using TBtools (version 2.096). Furthermore, TBtools searched the sorghum whole-genome database to retrieve a 2000 bp nucleotide sequence upstream of the *SbCalS* gene's start codon (ATG) [43]. Subsequent analysis of the sequence was carried out using the PlantCARE online tool (<https://bioinformatics.psb.ugent.be/webtools/plantcare/html/>, accessed on 10 March 2024) to predict cis-acting elements in *SbCalS* of sorghum [44]. Finally, TBtools (version 2.096) was used to visualize the conserved motifs, gene structure, and cis-acting elements information [43].

2.5. Chromosomal Mapping and Intraspecific Collinearity and *Ka/Ks* Value Analysis of *SbCalS* Gene Family

Using the sorghum genome and annotation files downloaded from NCBI [45], the chromosome length file was generated by inputting the relevant files into the Fasta Stats tool within the TBtools suite as directed. To derive the gene density file, we employed the Gene Density Profile tool and utilized One Step MCScanX to produce the intraspecific collinearity file for sorghum. The Advanced Circos tool was used to create visualizations of chromosome localization and collinearity relationships, which were subsequently refined using Adobe Illustrator (2023). Genes were designated as *SbCalS1* through *SbCalS11* according to their chromosomal locations. The Simple *Ka/Ks* Calculator (NG) within TBtools was used to compute the non-synonymous (*Ka*) and synonymous (*Ks*) substitution

rates for the genes (Table S1) [43], with Ka/Ks ratios indicating positive evolution when greater than 1, negative evolution when less than 1, and neutral evolution when equal to 1 [46].

2.6. Interspecific Collinearity Analysis of *SbCalS* and Construction of Phylogenetic Tree

Using the One Step MCScanX tool with default parameters in the TBtools toolbox [47], collinearity files between sorghum, maize, and rice were obtained. Subsequently, the Multiple Synteny Plot tool was used to generate plots, and Adobe Illustrator (2023) was used for aesthetic enhancement. The neighbor-joining (NJ) method in MEGA11 software (version 11.0.13) was applied to construct an evolutionary tree for the callose gene families of sorghum, maize, and rice. To ensure data accuracy, bootstrap replications were set to 1000 [48]. Finally, the evolutionary tree was beautified using iTOLv6 (version 6.8.2) (<https://itol.embl.de/>, accessed on 12 March 2024) [49].

2.7. Analysis of the *SbCalS* Gene Family Using Published RNA-Seq Data

Publicly available sorghum transcriptome data were downloaded from NCBI to assess the specific expression of the sorghum *CalS* gene family under aphid infestation (PR-JNA716317) [50,51]. To ensure the quality of the Fastq data, the FastQC software (version 0.12.1) (<https://github.com/s-andrews/FastQC>, accessed on 20 March 2024) was utilized. Subsequently, Trimmomatic software (version 0.40) was employed to remove duplicates and low-quality sequences, resulting in clean, filtered data [52]. The filtered data were then processed using the Kallisto Super Wrapper V3 package within the TBtools toolkit. Finally, differential gene expression was analyzed using the HeatMap plugin in TBtools [53].

2.8. Expression Characteristics of *SbCalS* Genes under Aphid Infestation

Sampling was performed at the early stages (6 h, 24 h, 48 h) and the late stage (7 d) after aphid infestation in sorghum. Samples were also taken at 0 h and 7 d from uninfested plants to serve as controls for the early and late stages. These samples were used for RNA extraction, following the method described in reference [54]. Primers for qPCR targeting *SbCalS* genes were designed using Premier 6 software (Table S2). The sorghum endogenous control gene was referenced from the study by J Li et al. [55]. Primer specificity was verified using Primer-BLAST (https://www.ncbi.nlm.nih.gov/tools/primer-blast/index.cgi?LINK_LOC=BlastHome, accessed on 25 March 2024) [56]. The qPCR experiments were conducted according to the method of Jin et al. [57]. PCR was conducted on an ABI ViiA 7 Real-Time PCR System (Life Technologies, Carlsbad, CA, USA), and data were analyzed using the $2^{-\Delta\Delta C_t}$ method [58]. Statistical analysis and data visualization were performed using GraphPad Prism 8 software. Each qPCR reaction included three technical replicates [59].

2.9. Determination of Callose Content in Sorghum

To investigate the effect of callose content on aphids, we selected the highly resistant sorghum HX133 and the susceptible sorghum HX141. We inoculated the leaves with ten third- to fourth-instar aphids and recorded the number of aphids daily for 7 days. The experiment was conducted in a climate-controlled chamber with a photoperiod of 16 h light and 8 h dark, a temperature of 28 °C, and relative humidity of 50–60%. Sampling was performed at the early stages (6 h, 24 h, and 48 h) and the later stage (7 d) after aphid infestation. We used the Plant Callose ELISA KIT from Shanghai Yuanye Bio-Technology Co., Ltd., Shanghai, China, following the manufacturer's instructions meticulously. The microplate reader used was the SpectraMax[®]190 from Molecular Devices Ltd., San Jose, CA, USA. All treatments in this experiment were replicated three times.

3. Results

3.1. Identification of *SbCalS* Gene Family

We identified 11 genes encoding callose synthase in the sorghum genome. These *SbCalS* genes were annotated using the SMART website, and all of them contained both callose synthase and Fks1 domains. Among the 11 *SbCalS* genes, 7 contained the Vta1 domain (Figure 2). The callose synthase domain serves as a typical catalytic function (Figure S1), while the Vta1 domain is involved in transport to the vacuole, where it participates in sorting membrane proteins for degradation in the lysosome [60]. Fks1 is a type of β -1,3-glucan, and in the Fks1 structure, various lipid-binding and significant membrane distortions were observed, indicating Fks1's interaction with membranes [61]. To elucidate the relationship between the classification and structure of *SbCalS*, we conducted a determination of gene structure and conserved motifs in *SbCalS* proteins. Initially, a phylogenetic tree was constructed for the 11 *SbCalS* proteins in sorghum. Based on evolutionary relationships, *SbCalS* was categorized into three branches. Specifically, all Fks1 domains contained motifs 8 and 10, while the majority of glycosyltransferase domains contained motifs 7, 3, 6, 1, 4, 2, and 5. In the glycosyltransferase domain, the *SbCalS6* gene repeated motif 4, *SbCalS8* and *SbCalS10* had an additional motif 11, and *SbCalS3* lacked motif 6. Overall, conservation was relatively high in the Fks1 and glycosyltransferase domains, providing favorable evidence for the functional consistency among members of the *SbCalS* family.

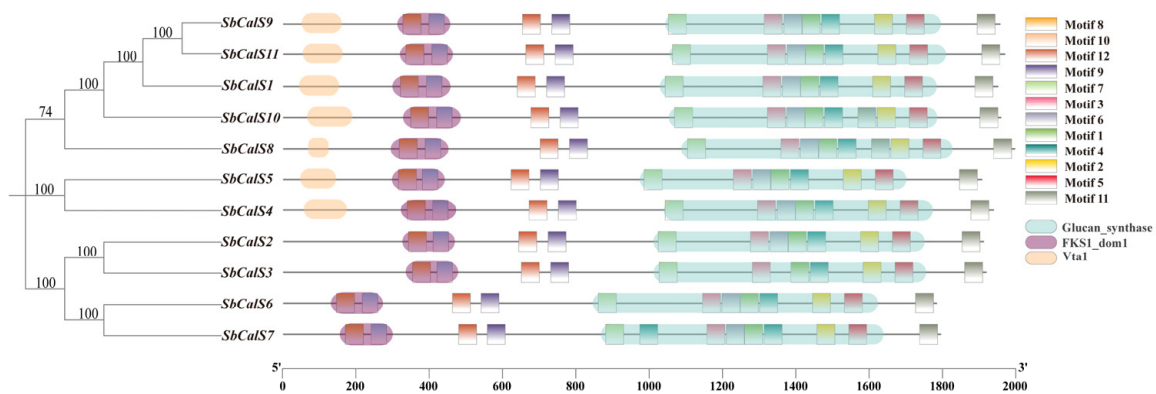


Figure 2. Conservation domain motif binding diagram of the *SbCalS* gene family.

3.2. Chromosome Localization and Intraspecific Colinear and *Ka/Ks* Analysis of *SbCalS* Gene Family

With the sorghum genome database, we identified 11 members of the *SbCalS* family, named sequentially according to their chromosomal locations from top to bottom and left to right. The 11 *SbCalS* were assigned to chromosomes 1, 3, 4, and 10 of sorghum (Figure 3). Specifically, *SbCalS1*, *SbCalS2*, and *SbCalS3* are located on chromosome 1; *SbCalS4*, *SbCalS5*, *SbCalS6*, and *SbCalS7* reside are located on chromosome 3; *SbCalS8* and *SbCalS9* are positioned on chromosome 4; and *SbCalS10* and *SbCalS11* are on chromosome 10. No tandem gene duplication events were observed in the *SbCalS* family, with only one pair of *SbCalS* genes undergoing segmental duplication. It was found that the *Ka/Ks* ratio of *SbCalS* < 1, indicating negative selection pressure acting on the gene family members. The approximate age of gene duplication events was estimated using the equation $T = Ks/(2\lambda)$ ($\lambda = 6.5 \times 10^{-9}$) [62]. Based on the data, the first segmental duplication event of this gene pair likely occurred approximately 76.42 million years ago, indicating that this segmental duplication happened after the origin of sorghum [63].

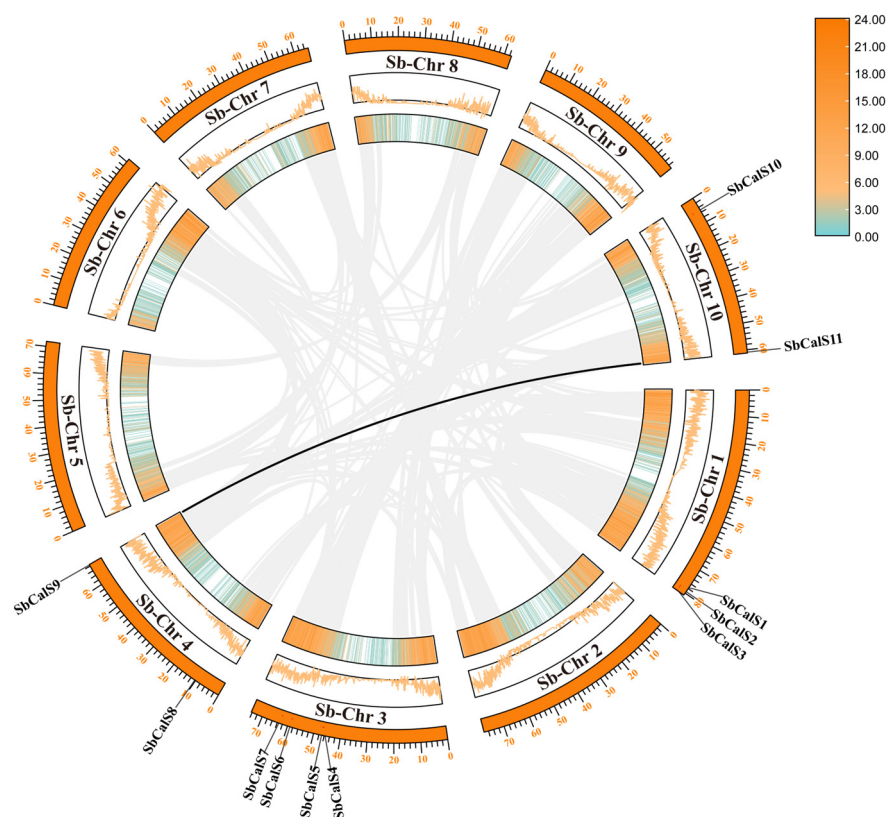


Figure 3. Chromosomal mapping of *SbCalS* gene and intraspecific collinearity analysis of sorghum. The innermost circle represents chromosome gene density. Higher gene density is indicated by the color orange and taller peaks, while lower gene density is indicated by the color blue and shorter peaks.

3.3. Physiochemical Properties and Subcellular Localization Analysis of *SbCalS* Gene Family

Based on the findings in (Table S3), *SbCalS* proteins range in length from 1779 to 1992 amino acids. The molecular weights (MW) of *SbCalS* proteins vary between 205,550.20 Da (*SbCalS6*) and 228,905.52 Da (*SbCalS8*), while their isoelectric points (pI) range from 8.54 (*SbCalS2*) to 9.34 (*SbCalS6*). The instability index ranges from 37.82 (*SbCalS1*) to 44.69 (*SbCalS8*), and the grand average of hydropathy (GRAVY) values range from -0.149 (*SbCalS4*) to -0.02 (*SbCalS5*), indicating that *SbCalS* is a hydrophilic protein containing 14–18 transmembrane domains. According to the subcellular localization prediction (Table S4), ten *SbCalS* proteins are located in the plasma membrane, with *SbCalS7* alone in the nucleus, suggesting possible involvement in callose synthesis regulation through coordination between different organelles, with the cell membrane being the primary workplace. Protein secondary structure mainly consists of α -helices, β -turns, irregular coils, and extended strands, which form the basis of protein tertiary structure. Different amino acid residues tend to form different secondary structure elements. This study determined that α -helices constitute the majority of the secondary structure in the 11 *SbCalS* amino acid sequences, indicating their predominant role in the protein's secondary structure.

3.4. Structural Analysis of the *SbCalS* Gene Family

We compared the exon-intron numbers, arrangement, and lengths of the 11 *SbCalS* genes and found significant differences (Figure 4). The number of exons ranged from 1 to 51. Gene structure diversity is a direct cause of protein diversity and contributes to their different functions. Both *SbCalS2* and *SbCalS3* possess 51 exons, yet their exon distributions differ significantly. *SbCalS6* and *SbCalS7* exhibit strikingly similar gene lengths, exon positions, and numbers. These findings suggest that variations in exon distribution and quantity may contribute to functional divergence [64].

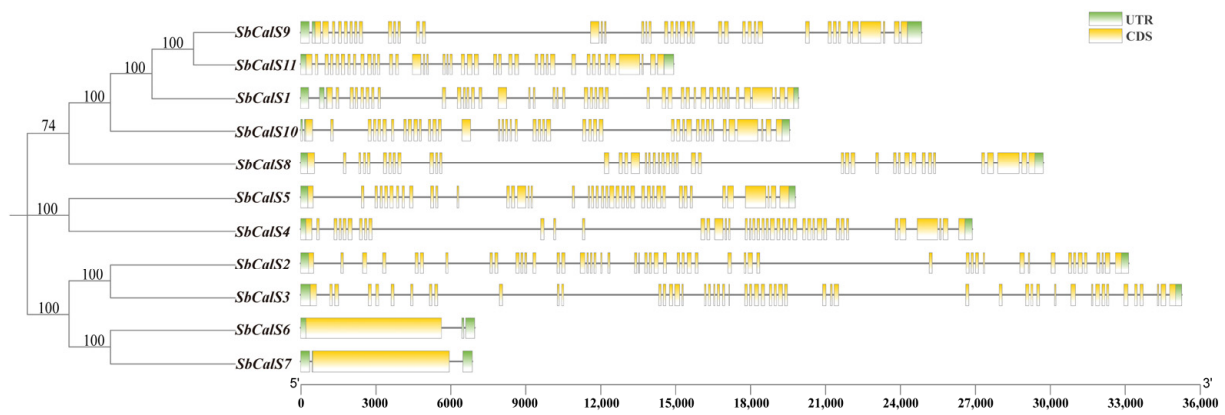


Figure 4. Gene structure of *SbCalS*. Exons are represented by yellow boxes, introns by black lines, and UTR regions by green boxes.

3.5. Cis-Acting Element Analysis of *SbCalS* Gene Family

The *CalS* gene is vital for resistance to both biotic and abiotic stresses and is potentially regulated by plant hormones. Analysis of the upstream 2000 bp region of *CalS* promoters (Figure 5A) revealed numerous plant hormone response elements, including those for MeJA (methyl jasmonate), ABA (abscisic acid), GA (gibberellin), Auxin, and SA. Elements associated with seed development were also found, including seed-specific regulatory elements and embryo-expressed cis-regulatory elements. Various factors associated with plant resistance were identified, including drought-inducible factors, anaerobic induction essential cis-regulatory elements, low-temperature responsive cis-acting elements, hypoxia-specific induction factors, and defense and stress-responsive cis-acting elements. Among these, the SA response element was the least abundant, while the three most prevalent elements were the MeJA response element, ABA response element, and anaerobic induction essential cis-regulatory element, in that order (Figure 5B). The *SbCalS* promoter region contains cis-acting elements that indicate its expression is regulated by multiple stress-related hormones and factors, contributing to the plant’s stress resistance and seed development.

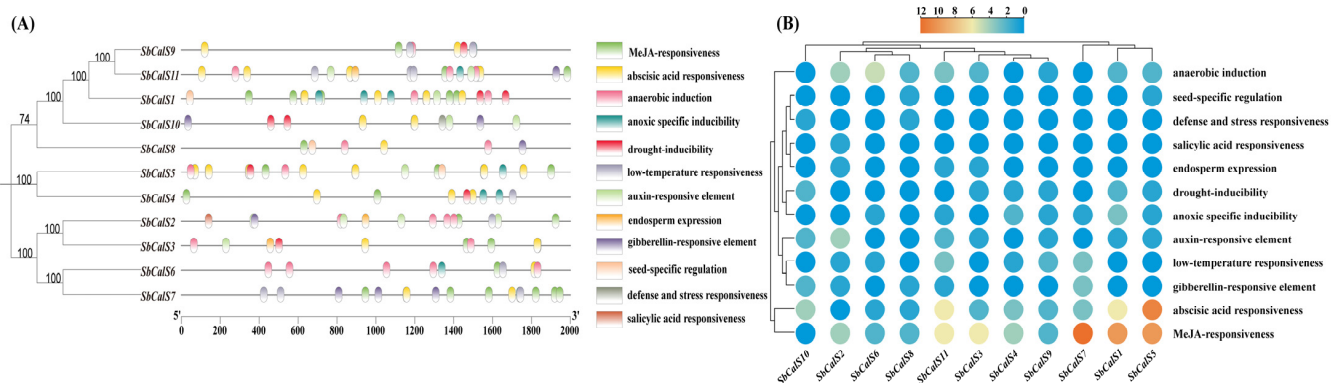


Figure 5. (A) Cis-acting elements of the *SbCalS* gene family; (B) Heat map of cis-acting elements of the *SbCalS* gene family. Orange indicates a high number of cis-regulatory element enrichments, while blue indicates a low number.

3.6. Analysis of *SbCalS* Interspecific Covariates and Phylogenetic Trees

Through retrieval from the NCBI database and detection using Smart and CDD programs, a total of 11 *SbCalS* genes were ultimately identified. Homologous callose genes from maize (*Zea mays* L.) and rice (*Oryza sativa* L.) were used, with each having ten callose genes [65]. To further elucidate the evolutionary relationships of the *SbCalS* genes, synteny and phylogenetic analyses were conducted among sorghum, rice, and maize. Using MEGA11 software (version 11.0.13), a phylogenetic tree of the *CalS* family

was constructed. As depicted in (Figure 6), the *CalS* genes were categorized into three sub-branches based on their homology. Sub-branch A contained the fewest *CalS* genes, with a total of 8 genes from the 3 species: 3 from sorghum, 3 from rice, and 2 from maize. Sub-branch B included 11 *CalS* genes: 4 from sorghum, 4 from maize, and 3 from rice. Sub-branch C had the highest number of *CalS* genes, with a total of 12, including 4 from each species. Overall, the number of *CalS* genes in each sub-branch from different species was relatively balanced, indicating a high degree of homology among the *CalS* genes of sorghum, maize, and rice. This suggests that *CalS* genes from the same sub-branch in different species may have similar functions and close evolutionary relationships. The synteny analysis, illustrated in (Figure 7) and created using TBtools, further supports this finding. The analysis revealed 17 pairs of homologous *CalS* genes, with 9 pairs between sorghum and maize, and 8 pairs between sorghum and rice. Although sorghum shares one more homologous *CalS* gene with maize than with rice, the overall high homology among the three species is evident. In conclusion, the high degree of homology and balanced distribution of *CalS* genes across the three species suggest that these genes likely share similar functions and have evolved closely, providing insights into their evolutionary relationships and functional conservation.

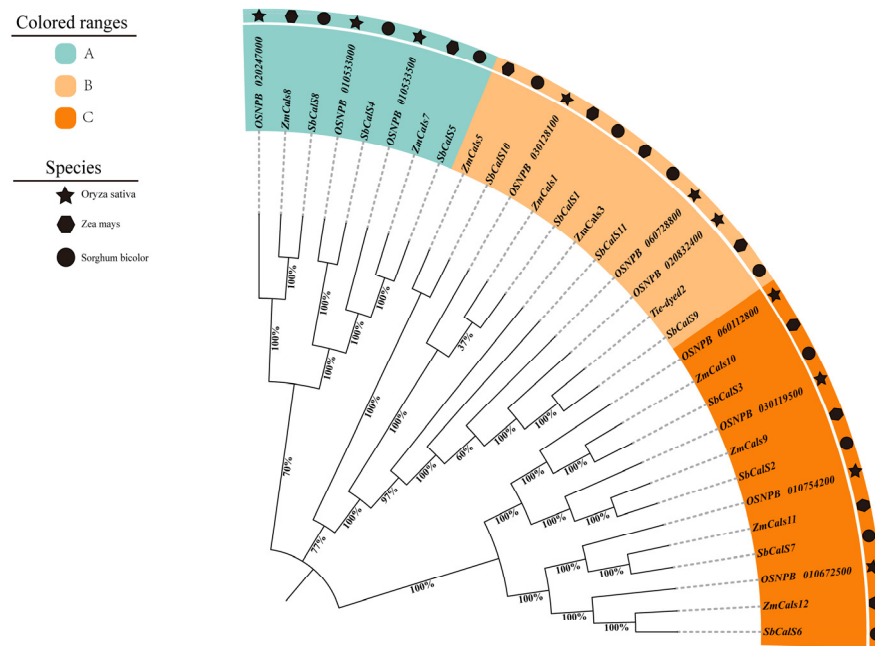


Figure 6. Evolutionary tree of *CalS* genes in sorghum, maize, and rice. Based on homology, they are classified into three subclades: A, B, and C, in ascending order.

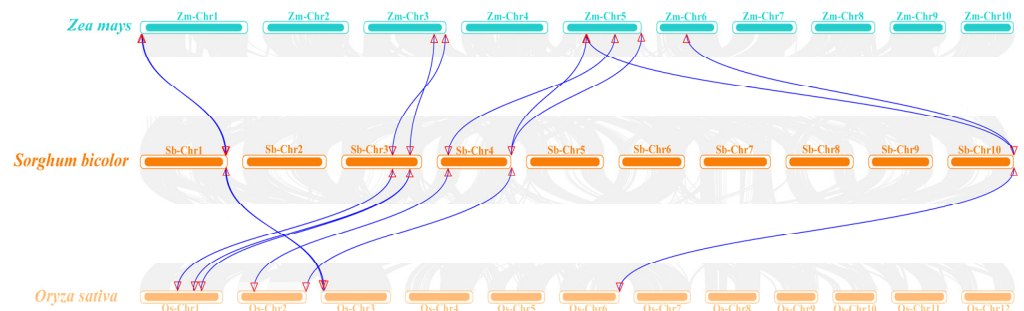


Figure 7. The homology of *CalS* genes among sorghum, maize, and rice is depicted, with blue lines indicating homologous *CalS* genes across different species and gray lines representing the synteny between other genes across these species.

3.7. Transcriptome Analysis of the *SbCalS* Gene Family Following Aphid Infestation

Using publicly available RNA-seq data from the NCBI transcriptome database [50], we analyzed the expression levels of the *SbCalS* gene family. A heatmap was constructed using hierarchical clustering, revealing differential expression patterns of the *CalS* genes in sorghum varieties in response to aphid infestation (Figure 8). Specifically, *SbCalS1*, *SbCalS7*, and *SbCalS8* exhibited higher expression levels at the early time points in all three sorghum varieties, but their expression decreased at the late time point. However, *SbCalS5* showed an increase in expression with the duration of aphid infestation in the resistant variety, reaching its highest level at 7 days post-infestation, with minimal changes observed in the reference and susceptible varieties. *SbCalS11* consistently exhibited low expression levels across all treatments.

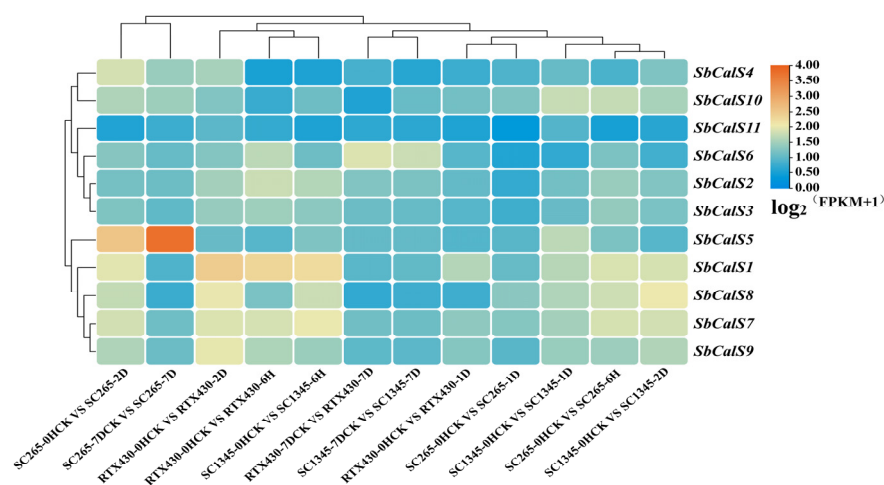


Figure 8. Differential expression of the *SbCalS* gene family transcriptome under aphid infestation. RTx430 served as the reference sorghum, SC265 served as the resistant sorghum, and SC1345 served as the susceptible sorghum. Sampling occurred at early time points (6 h, 24 h, and 48 h) and a late time point (7 d) following aphid infestation, with samples collected from non-infested plants at 0 h and 7 d serving as controls. Genes demonstrating high expression levels were indicated in orange, while those displaying low expression levels were marked in blue.

3.8. Expression Pattern Analysis of the *SbCalS* Gene Family Following Aphid Infestation

To elucidate the role of the *SbCalS* gene family in response to aphid infestation, we subjected the highly resistant variety HX133 and the susceptible variety HX141 to aphid stress induction. The results are depicted in (Figure 9). *SbCalS1* and *SbCalS2* exhibited similar expression patterns, showing significant expression in the early stages of resistance and susceptibility, respectively. At 6 h post-aphid stress induction, HX133 displayed heightened sensitivity compared to HX141, which showed no significant difference from the control. While *SbCalS1* gradually downregulated in the later stages, *SbCalS2*, particularly in HX133, exhibited significant upregulation. *SbCalS3* and *SbCalS9* showed no significant difference in expression between resistant and susceptible sorghum. In *SbCalS6*, HX141 consistently exhibited higher expression levels throughout the time course compared to HX133. For *SbCalS8* and *SbCalS10*, HX141 displayed slightly higher expression levels in the early stages compared to HX133, but in the later stages, particularly for *SbCalS10*, HX133 surpassed HX141 by 2.16-fold. The major differences were observed in *SbCalS5*, *SbCalS7*, and *SbCalS11*, where the expression levels of HX133 and HX141 exhibited two extreme patterns throughout the entire stage. HX133 showed significant downregulation in the early stages, while HX141 exhibited significant upregulation, especially in *SbCalS11*, where it was upregulated by 6.8-fold at 24 h. In the later stages, HX141 showed significant downregulation, while HX133 displayed notable upregulation. Notably, the expression of *SbCalS5* was markedly upregulated by 4.4-fold, consistent with the aforementioned RNA-seq data. *SbCalS4* exhibited similar early-stage expression patterns to *SbCalS5*, *SbCalS7*,

and *SbCals11*, but in the later stages, the upregulation in HX141 was more pronounced compared to HX133.

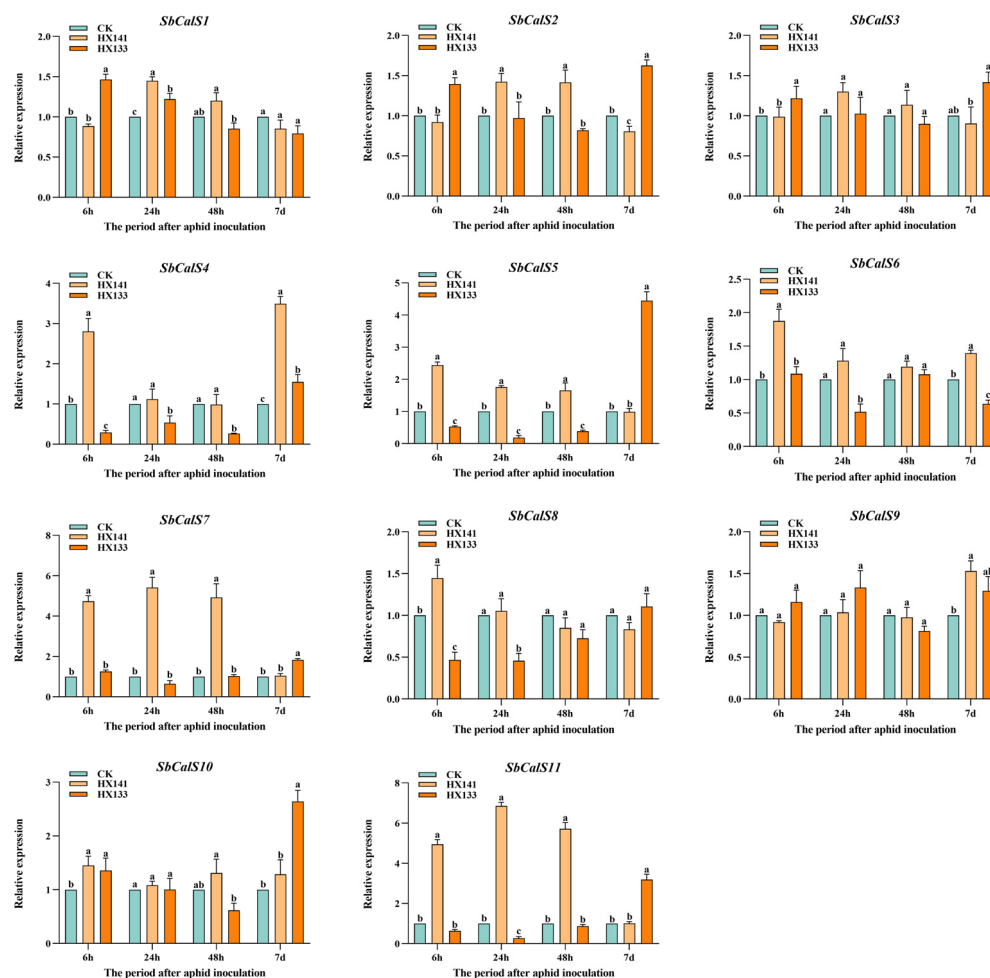


Figure 9. Expression patterns of the *SbCals* gene family following aphid infestation. The infestation times were set at four early time points (0, 6, 24, and 48 h post-infestation), with 0 h serving as the early control, and one late time point at 7 days post-infestation, with uninfested plants at 7 days serving as the control. Significant differences are denoted by lowercase letters ($p < 0.05$).

3.9. Analysis of Sorghum Aphid Population and Callose Content

To further explore the function of callose in sorghum, I evaluated the aphid populations and callose levels in different sorghum varieties. The findings indicated that in HX141, the aphid population increased continuously, reaching its peak at 6 days, followed by a decline on the 7th day, primarily due to sorghum wilting. In contrast, the aphid population growth rate in HX133 was significantly slower than in HX141 and stabilized between 4 and 7 days (Figure 10A). Upon measuring the callose levels, it was evident that HX133 had a markedly higher callose content compared to HX141 (Figure 10B). At 6 h post-aphid infestation, HX133 exhibited an increase in callose content, whereas HX141 showed no significant change, suggesting a quicker defense response in HX133. The pattern observed in HX141 was similar to the control, implying that HX141 is not highly responsive to aphid feeding. Nevertheless, in the initial stages of aphid infestation, both sorghum varieties exhibited higher callose levels than the control group, indicating that aphid feeding triggers an increase in callose production.

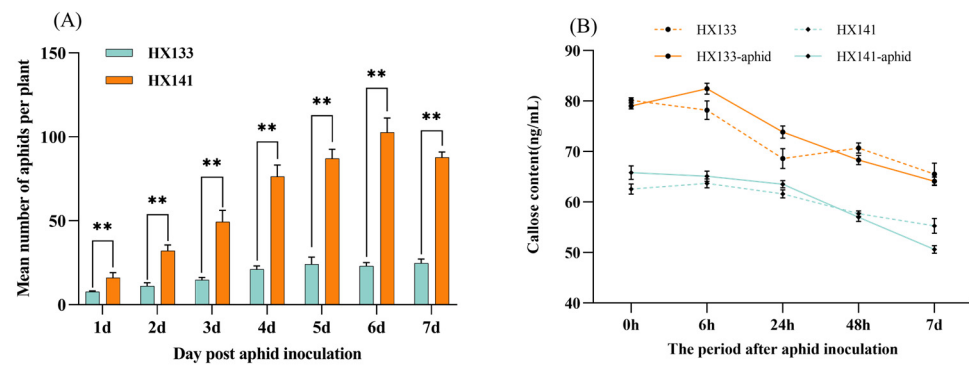


Figure 10. Differences in the number of aphids and the content of callose in resistant sorghum. Panel (A) shows the difference in the number of aphids 7 days post-infestation (** $p < 0.01$). Panel (B) displays the differences in callose content at four early time points (0, 6, 24, and 48 h) and one late time point (7 days) post-infestation, with the dashed line indicating the control group.

4. Discussion

4.1. The Role and Mechanism of the CalS Gene Family in Plant Defense

Over 120 years ago, callose was reported as an important component of the cell wall [66]. The cell wall acts as the primary defense against environmental and biological stresses. Regulating callose synthase can result in the formation of protrusive structures on the cell wall, which effectively prevents the infiltration of parasitic microorganisms. Although recent advances in molecular and genetic techniques have led to studies on the role of callose and the regulation of callose synthase activity in bacteria, yeast, and plants, many aspects remain to be explored [10]. Callose is widely present in the intercellular matrix as well as in the cells of leaves and stems [67], controlling molecular transport and regulating plasmodesmata transport. External environmental changes and pest invasions are the main causes of callose accumulation, controlled by various signaling pathways. In some plants, calcium ions and phosphoproteins also appear to be involved in the regulation of callose synthesis [68]. The callose synthase complex is found in at least two distinct forms across various tissues and interacts with membrane proteins, UDP-glucose transferases, Rop1, and potentially other membrane-associated proteins [69]. Currently, the structural synthesis and regulatory mechanisms of callose synthase are not yet fully understood.

4.2. The Multiple Roles and Regulation of the CalS Gene Family in Plants

Callose is found in almost all plant tissues and is crucial at various stages of plant growth and development [10]. The members of the callose synthase gene family differ among different plants. In *Paeonia lactiflora*, there are 8 *CalS* genes [70]; in rice and maize, there are 10 *CalS* genes; in *Arabidopsis thaliana*, there are 12 *CalS* genes; and in this study, 11 *SbCalS* genes were identified. The observed differences are likely due to gene loss during the evolution from *Arabidopsis thaliana* to angiosperms like rice and *Paeonia lactiflora*. We propose that the functions of callose synthase gene family members have diversified. For instance, *GSL2* is essential for callose synthesis in *Arabidopsis thaliana*, especially in the exine of pollen walls, and *CalS5* gene knockout mutants show significant fertility reduction [71]. In *Arabidopsis thaliana*, the *GSL1* and *GSL5* genes collaboratively contribute to the formation of the callose wall, playing a crucial role in pollen development [72]. Qunkai Niu et al. found that the *ZmCals5*, *ZmCals10*, and *ZmCals12* genes are expressed in maize anthers and pollen, suggesting a potential collaborative role in reproductive development [65]. In rice, the expression of *OsGSL5* is downregulated in *Osspl* (*OsSPOROXYTELESS*) mutants, leading to defects in callose deposition in the male-sterile anthers [73]. Therefore, the mechanisms and functions of interactions among callose synthase gene family members remain to be further studied.

The deposition of callose is of significant importance in the cell wall's defense against pathogens and pests. Different *Chrysanthemum morifolium* varieties

were inoculated with Chrysanthemum stunt virus (CSVd) [74], and the intercellular callose content in resistant varieties was significantly higher than in susceptible ones. This suggests that callose deposition is a defense mechanism against pathogens. When different resistance levels of *Brassica napus* were inoculated with *Leptosphaeria maculans*, it was found that callose deposition in susceptible canola gradually dispersed over time, whereas it remained relatively constant in resistant canola [75]. The brown planthopper's (*Nilaparvata lugens*) effector NIG14 can stimulate the production of reactive oxygen species, which subsequently promotes callose accumulation [76]. Mengjing Sun et al. found that, in screening resistant and susceptible peppers (*Capsicum* spp.), callose deposition was detected in varieties resistant to the green peach aphid (*Myzus persicae*), but not in susceptible varieties [77].

In the regulation of callose synthase, plant hormones are believed to play a crucial role. Auxin [78], ABA [79], GA, and SA [80] regulate the expression of callose synthase. In our study, it was found that cis-acting elements related to JA, ABA, and GA were more abundant. Treatment of sorghum seedlings with JA revealed that JA-induced plant defense responses effectively prevented aphid infestation [81]. Exogenous application of JA can induce the expression of *CmAOS* and *CmCOI1* in Chrysanthemum, thereby enhancing aphid resistance [82]. In cases where fungal pathogens penetrate or sap-feeding pests pierce plant tissues, cell wall deposition materials can form rings or protrusions, with callose being a major component [83]. SA and ABA can influence the deposition of callose in intercellular spaces [66]. V. Repka et al. found that JA can also induce callose deposition in grapevine leaves [84]. Recent studies have shown that transient overexpression of *CsCalS11* in citrus enhances callose deposition [85]. According to previous studies, JA and ABA play significant roles in resisting both biotic and abiotic stresses. [86,87]. Most plant defenses against herbivorous insects are induced by mechanical damage and saliva [88]. Mechanical damage can trigger phloem and xylem electrical signals, leading to an increase in cytosolic calcium ion concentration [89]. Wang et al. identified a dominant aphid-resistant major gene, *RMES1*, in the Chinese sorghum variety HN16, which confers resistance to sorghum aphids [90]. Interestingly, Puri et al. discovered a close relationship between the *RMES1* gene and the formation of callose. The *RMES1* gene may influence the synthesis and deposition of callose by regulating Ca^{2+} signaling pathways, thereby enhancing plant resistance [91]. In summary, plant defense is a complex regulatory network. Additionally, plant hormones play a crucial role in the regulation of callose deposition. Callose deposition is vital in sorghum's defense mechanism against aphids, yet its regulation and mediation mechanisms require further validation and exploration.

5. Conclusions

We have identified 11 *CalS* genes in the sorghum genome, which are unevenly distributed across four chromosomes. Interspecies collinearity analysis revealed a close phylogenetic relationship among sorghum, maize, and rice. The cis-acting elements in sorghum *CalS* genes include numerous plant hormones, defense, and stress response elements. qPCR analysis showed significant changes in the expression of *SbCalS5*, *SbCalS7*, and *SbCalS11* genes under aphid stress. Additionally, we assessed callose content, discovering that HX133 sorghum exhibited significantly higher levels compared to the susceptible HX141 variety. Integrating transcriptome data with cis-acting element analysis, we propose that the *SbCalS5* gene plays a pivotal role in sorghum's defense against aphids. Although this study does not extensively investigate the regulation and molecular mechanisms of the *SbCalS* gene, it lays the groundwork for future research into the function of the sorghum *CalS* gene family in aphid resistance.

Supplementary Materials: The following supporting information can be downloaded at: <https://www.mdpi.com/article/10.3390/agronomy14071393/s1>, Figure S1: The multiple sequence alignment of conserved domains in *SbCalS* gene family; Table S1: *SbCalS* protein ka/ks values; Table S2: Primers used for qPCR of the *SbCalS* gene family; Table S3: Analysis of the Physicochemical Properties and Subcellular Localization of the *SbCalS* Gene Family; Table S4: Secondary structure and predicted signal peptide of *CalS* protein in Sorghum.

Author Contributions: Conceptualization, D.W. and J.D.; methodology, D.W.; software, K.Z., Y.L., and T.W.; validation, T.W., M.G., X.L. and H.Y.; formal analysis, J.L.; investigation, K.Z. and T.W.; resources, D.W. and J.D.; data curation, K.Z., T.W. and Y.L.; writing—original draft preparation, K.Z., Y.L., T.W., M.G., X.L., H.Y., J.D. and D.W.; writing—review and editing, K.Z., Y.L., H.Y., J.D. and D.W.; visualization, K.Z. and T.W.; supervision, D.W. and J.D.; project administration, K.Z.; funding acquisition, D.W., J.D. and H.Y. All authors have read and agreed to the published version of the manuscript.

Funding: This research was funded by the Natural Science Foundation of Education Department of Anhui Province (2023AH051852), the Anhui Province International Joint Research Center of Forage Bio-breeding (No.AHIJRCFB202303), the Key Discipline Construction Funds for Crop Science of Anhui Sciences and Technology University (No.XK-XJGF001), the Transformation of high-yielding and stress-resistant corn varieties and precision cultivation technology for high planting density (No.2024ZH017), and the Anhui Province Agricultural Germplasm Resource Bank (Nursery) Performance Award Project (Anhui Province Maize Germplasm Resource Bank No.1025).

Data Availability Statement: The data presented in this study are available on request from the corresponding author.

Acknowledgments: The authors would like to thank Anhui Science and Technology University for supporting this study.

Conflicts of Interest: The authors declare no conflicts of interest.

References

- Begna, T. Role of sorghum genetic diversity in tackling drought effect in Ethiopia. *Int. J. Adv. Res. Biol. Sci.* **2021**, *8*, 29–45.
- Afify, A.E.-M.M.; El-Beltagi, H.S.; Abd El-Salam, S.M.; Omran, A.A. Bioavailability of iron, zinc, phytate and phytase activity during soaking and germination of white sorghum varieties. *PLoS ONE* **2011**, *6*, e25512. [[CrossRef](#)] [[PubMed](#)]
- Taleon, V.; Dykes, L.; Rooney, W.; Rooney, L. Effect of genotype and environment on flavonoid concentration and profile of black sorghum grains. *J. Cereal Sci.* **2012**, *56*, 470–475. [[CrossRef](#)]
- Kim, J.-S.; Hyun, T.K.; Kim, M.-J. The inhibitory effects of ethanol extracts from sorghum, foxtail millet and proso millet on α -glucosidase and α -amylase activities. *Food Chem.* **2011**, *124*, 1647–1651. [[CrossRef](#)]
- Abd Elmoneim, O.E.; Schiffler, B.; Bernhardt, R. Effect of fermentation on the functional properties of sorghum flour. *Food Chem.* **2005**, *92*, 1–5.
- Gordy, J.W.; Brewer, M.J.; Bowling, R.D.; Buntin, G.D.; Seiter, N.J.; Kerns, D.L.; Reay-Jones, F.P.; Way, M. Development of economic thresholds for sugarcane aphid (Hemiptera: Aphididae) in susceptible grain sorghum hybrids. *J. Econ. Entomol.* **2019**, *112*, 1251–1259. [[CrossRef](#)]
- Bowling, R.D.; Brewer, M.J.; Kerns, D.L.; Gordy, J.; Seiter, N.; Elliott, N.E.; Buntin, G.D.; Way, M.; Royer, T.; Biles, S. Sugarcane aphid (Hemiptera: Aphididae): A new pest on sorghum in North America. *J. Integr. Pest Manag.* **2016**, *7*, 12. [[CrossRef](#)] [[PubMed](#)]
- Singh, B.; Padmaja, P.; Seetharama, N. Biology and management of the sugarcane aphid, *Melanaphis sacchari* (Zehntner)(Homoptera: Aphididae), in sorghum: A review. *Crop Prot.* **2004**, *23*, 739–755. [[CrossRef](#)]
- Narayana, D. Screening for aphids and sooty molds in sorghum. *Sorghum Newsl.* **1975**, *18*, 21–22.
- Li, N.; Lin, Z.; Yu, P.; Zeng, Y.; Du, S.; Huang, L.-J. The multifarious role of callose and callose synthase in plant development and environment interactions. *Front. Plant Sci.* **2023**, *14*, 1183402. [[CrossRef](#)]
- Chen, X.-Y.; Kim, J.-Y. Callose synthesis in higher plants. *Plant Signal. Behav.* **2009**, *4*, 489–492. [[CrossRef](#)] [[PubMed](#)]
- Caillaud, M.-C.; Wirthmueller, L.; Sklenar, J.; Findlay, K.; Piquerez, S.J.; Jones, A.M.; Robatzek, S.; Jones, J.D.; Faulkner, C. The plasmodesmal protein PDL1 localises to haustoria-associated membranes during downy mildew infection and regulates callose deposition. *PLoS Pathog.* **2014**, *10*, e1004496. [[CrossRef](#)] [[PubMed](#)]
- Blümke, A.; Somerville, S.C.; Voigt, C.A. Transient expression of the Arabidopsis thaliana callose synthase PMR4 increases penetration resistance to powdery mildew in barley. *Adv. Biosci. Biotechnol.* **2013**, *2013*, 35416.
- Sanmartín, N.; Pastor, V.; Pastor-Fernández, J.; Flors, V.; Pozo, M.J.; Sánchez-Bel, P. Role and mechanisms of callose priming in mycorrhiza-induced resistance. *J. Exp. Bot.* **2020**, *71*, 2769–2781. [[CrossRef](#)]
- Kim, S.-Y.; Bengtsson, T.; Olsson, N.; Hot, V.; Zhu, L.-H.; Åhman, I. Mutations in two aphid-regulated β -1, 3-glucanase genes by CRISPR/Cas9 do not increase barley resistance to *Rhopalosiphum padi* L. *Front. Plant Sci.* **2020**, *11*, 538516. [[CrossRef](#)] [[PubMed](#)]
- Kim, J.H.; Jander, G. Myzus persicae (green peach aphid) feeding on Arabidopsis induces the formation of a deterrent indole glucosinolate. *Plant J.* **2007**, *49*, 1008–1019. [[CrossRef](#)] [[PubMed](#)]
- Botha, C.E.; Matsiliza, B. Reduction in transport in wheat (*Triticum aestivum*) is caused by sustained phloem feeding by the Russian wheat aphid (*Diuraphis noxia*). *S. Afr. J. Bot.* **2004**, *70*, 249–254. [[CrossRef](#)]
- Yao, L.; Zhong, Y.; Wang, B.; Yan, J.; Wu, T. BABA application improves soybean resistance to aphid through activation of phenylpropanoid metabolism and callose deposition. *Pest Manag. Sci.* **2020**, *76*, 384–394. [[CrossRef](#)] [[PubMed](#)]

19. Mbiza, N.I.T.; Hu, Z.; Zhang, H.; Zhang, Y.; Luo, X.; Wang, Y.; Wang, Y.; Liu, T.; Li, J.; Wang, X. GhCalS5 is involved in cotton response to aphid attack through mediating callose formation. *Front. Plant Sci.* **2022**, *13*, 892630. [[CrossRef](#)]
20. Zhang, Y.; Zhang, Y.; Chen, A.; Huo, R.; Yan, H.; Zhang, Z.; Guo, H. Callose deposition regulates differences in cotton aphid resistance among six watermelon varieties. *J. Pest Sci.* **2024**, 1–16. [[CrossRef](#)]
21. Barratt, D.P.; Kölling, K.; Graf, A.; Pike, M.; Calder, G.; Findlay, K.; Zeeman, S.C.; Smith, A.M. Callose synthase GSL7 is necessary for normal phloem transport and inflorescence growth in Arabidopsis. *Plant Physiol.* **2011**, *155*, 328–341. [[CrossRef](#)] [[PubMed](#)]
22. Wu, S.-W.; Kumar, R.; Iswanto, A.B.B.; Kim, J.-Y. Callose balancing at plasmodesmata. *J. Exp. Bot.* **2018**, *69*, 5325–5339. [[CrossRef](#)] [[PubMed](#)]
23. Yi, S.Y.; Shirasu, K.; Moon, J.S.; Lee, S.-G.; Kwon, S.-Y. The activated SA and JA signaling pathways have an influence on flg22-triggered oxidative burst and callose deposition. *PLoS ONE* **2014**, *9*, e88951. [[CrossRef](#)] [[PubMed](#)]
24. Ellinger, D.; Voigt, C.A. Callose biosynthesis in Arabidopsis with a focus on pathogen response: What we have learned within the last decade. *Ann. Bot.* **2014**, *114*, 1349–1358. [[CrossRef](#)] [[PubMed](#)]
25. Nalam, V.; Louis, J.; Shah, J. Plant defense against aphids, the pest extraordinaire. *Plant Sci.* **2019**, *279*, 96–107. [[CrossRef](#)] [[PubMed](#)]
26. Singh, A.; Sagar, S.; Biswas, D.K. Calcium dependent protein kinase, a versatile player in plant stress management and development. *Crit. Rev. Plant Sci.* **2017**, *36*, 336–352. [[CrossRef](#)]
27. Molina-Moya, E.; Terrón-Camero, L.C.; Pescador-Azofra, L.; Sandalio, L.M.; Romero-Puertas, M.C. Reactive oxygen species and nitric oxide production, regulation and function during defense response. In *Reactive Oxygen, Nitrogen and Sulfur Species in Plants: Production, Metabolism, Signaling and Defense Mechanisms*; John Wiley & Sons Ltd.: Hoboken, NJ, USA, 2019; pp. 573–590.
28. Kuśnierczyk, A.; Winge, P.; Jørstad, T.S.; TrocZYńska, J.; Rossiter, J.T.; Bones, A.M. Towards global understanding of plant defence against aphids—timing and dynamics of early Arabidopsis defence responses to cabbage aphid (*Brevicoryne brassicae*) attack. *Plant Cell Environ.* **2008**, *31*, 1097–1115. [[CrossRef](#)] [[PubMed](#)]
29. Zhang, J.; Li, Y.; Bao, Q.; Wang, H.; Hou, S. Plant elicitor peptide 1 fortifies root cell walls and triggers a systemic root-to-shoot immune signaling in Arabidopsis. *Plant Signal. Behav.* **2022**, *17*, 2034270. [[CrossRef](#)] [[PubMed](#)]
30. O'Lexy, R.; Kasai, K.; Clark, N.; Fujiwara, T.; Sozzani, R.; Gallagher, K.L. Exposure to heavy metal stress triggers changes in plasmodesmatal permeability via deposition and breakdown of callose. *J. Exp. Bot.* **2018**, *69*, 3715–3728. [[CrossRef](#)]
31. Tetreault, H.M.; Grover, S.; Scully, E.D.; Gries, T.; Palmer, N.A.; Sarath, G.; Louis, J.; Sattler, S.E. Global responses of resistant and susceptible sorghum (*Sorghum bicolor*) to sugarcane aphid (*Melanaphis sacchari*). *Front. Plant Sci.* **2019**, *10*, 426693. [[CrossRef](#)]
32. Hong, Z.; Delauney, A.J.; Verma, D.P.S. A cell plate-specific callose synthase and its interaction with phragmoplastin. *Plant Cell* **2001**, *13*, 755–768. [[PubMed](#)]
33. Bolser, D.M.; Staines, D.M.; Perry, E.; Kersey, P.J. Ensembl plants: Integrating tools for visualizing, mining, and analyzing plant genomic data. In *Plant Genomics Databases: Methods and Protocols*; Springer: Berlin/Heidelberg, Germany, 2017; pp. 1–31.
34. Finn, R.D.; Bateman, A.; Clements, J.; Coghill, P.; Eberhardt, R.Y.; Eddy, S.R.; Heger, A.; Hetherington, K.; Holm, L.; Mistry, J. Pfam: The protein families database. *Nucleic Acids Res.* **2014**, *42*, D222–D230. [[CrossRef](#)] [[PubMed](#)]
35. Marchler-Bauer, A.; Derbyshire, M.K.; Gonzales, N.R.; Lu, S.; Chitsaz, F.; Geer, L.Y.; Geer, R.C.; He, J.; Gwadz, M.; Hurwitz, D.I. CDD: NCBI's conserved domain database. *Nucleic Acids Res.* **2015**, *43*, D222–D226. [[CrossRef](#)] [[PubMed](#)]
36. Kb, N. GeneDoc: Analysis and visualization of genetic variation. *EMBnet News* **1997**, *4*, 1–4.
37. Letunic, I.; Bork, P. 20 years of the SMART protein domain annotation resource. *Nucleic Acids Res.* **2018**, *46*, D493–D496. [[CrossRef](#)] [[PubMed](#)]
38. Horton, P.; Park, K.-J.; Obayashi, T.; Fujita, N.; Harada, H.; Adams-Collier, C.; Nakai, K. WoLF PSORT: Protein localization predictor. *Nucleic Acids Res.* **2007**, *35*, W585–W587. [[CrossRef](#)] [[PubMed](#)]
39. Geourjon, C.; Deleage, G. SOPMA: Significant improvements in protein secondary structure prediction by consensus prediction from multiple alignments. *Bioinformatics* **1995**, *11*, 681–684. [[CrossRef](#)] [[PubMed](#)]
40. Petersen, T.N.; Brunak, S.; Von Heijne, G.; Nielsen, H. SignalP 4.0: Discriminating signal peptides from transmembrane regions. *Nat. Methods* **2011**, *8*, 785–786. [[CrossRef](#)] [[PubMed](#)]
41. Hallgren, J.; Tsirigos, K.D.; Pedersen, M.D.; Almagro Armenteros, J.J.; Marcatili, P.; Nielsen, H.; Krogh, A.; Winther, O. DeepTMHMM predicts alpha and beta transmembrane proteins using deep neural networks. *bioRxiv* **2022**. [[CrossRef](#)]
42. Bailey, T.L.; Johnson, J.; Grant, C.E.; Noble, W.S. The MEME suite. *Nucleic Acids Res.* **2015**, *43*, W39–W49. [[CrossRef](#)]
43. Chen, C.; Wu, Y.; Li, J.; Wang, X.; Zeng, Z.; Xu, J.; Liu, Y.; Feng, J.; Chen, H.; He, Y. TBtools-II: A “one for all, all for one” bioinformatics platform for biological big-data mining. *Mol. Plant* **2023**, *16*, 1733–1742. [[CrossRef](#)]
44. Lescot, M.; Déhais, P.; Thijs, G.; Marchal, K.; Moreau, Y.; Van de Peer, Y.; Rouzé, P.; Rombauts, S. PlantCARE, a database of plant cis-acting regulatory elements and a portal to tools for in silico analysis of promoter sequences. *Nucleic Acids Res.* **2002**, *30*, 325–327. [[CrossRef](#)] [[PubMed](#)]
45. Geer, L.Y.; Marchler-Bauer, A.; Geer, R.C.; Han, L.; He, J.; He, S.; Liu, C.; Shi, W.; Bryant, S.H. The NCBI biosystems database. *Nucleic Acids Res.* **2010**, *38*, D492–D496. [[CrossRef](#)]
46. Yadav, C.B.; Bonthala, V.S.; Muthamilarasan, M.; Pandey, G.; Khan, Y.; Prasad, M. Genome-wide development of transposable elements-based markers in foxtail millet and construction of an integrated database. *DNA Res.* **2015**, *22*, 79–90. [[CrossRef](#)]
47. Wang, Y.; Tang, H.; DeBarry, J.D.; Tan, X.; Li, J.; Wang, X.; Lee, T.-h.; Jin, H.; Marler, B.; Guo, H. MCScanX: A toolkit for detection and evolutionary analysis of gene synteny and collinearity. *Nucleic Acids Res.* **2012**, *40*, e49. [[CrossRef](#)] [[PubMed](#)]

48. Tamura, K.; Stecher, G.; Kumar, S. MEGA11: Molecular evolutionary genetics analysis version 11. *Mol. Biol. Evol.* **2021**, *38*, 3022–3027. [[CrossRef](#)]
49. Letunic, I.; Bork, P. Interactive Tree of Life (iTOL) v5: An online tool for phylogenetic tree display and annotation. *Nucleic Acids Res.* **2021**, *49*, W293–W296. [[CrossRef](#)]
50. Puri, H.; Grover, S.; Pingault, L.; Sattler, S.E.; Louis, J. Temporal transcriptomic profiling elucidates sorghum defense mechanisms against sugarcane aphids. *BMC Genom.* **2023**, *24*, 441. [[CrossRef](#)]
51. Sayers, E.W.; O'Sullivan, C.; Karsch-Mizrachi, I. Using GenBank and SRA. In *Plant Bioinformatics: Methods and Protocols*; Springer: Berlin/Heidelberg, Germany, 2022; pp. 1–25.
52. Bolger, A.M.; Lohse, M.; Usadel, B. Trimmomatic: A flexible trimmer for Illumina sequence data. *Bioinformatics* **2014**, *30*, 2114–2120. [[CrossRef](#)] [[PubMed](#)]
53. Chen, C.; Chen, H.; Zhang, Y.; Thomas, H.R.; Frank, M.H.; He, Y.; Xia, R. TBtools: An integrative toolkit developed for interactive analyses of big biological data. *Mol. Plant* **2020**, *13*, 1194–1202. [[CrossRef](#)]
54. Logemann, J.; Schell, J.; Willmitzer, L. Improved method for the isolation of RNA from plant tissues. *Anal. Biochem.* **1987**, *163*, 16–20. [[CrossRef](#)] [[PubMed](#)]
55. Li, J.; Fan, F.; Wang, L.; Zhan, Q.; Wu, P.; Du, J.; Yang, X.; Liu, Y. Cloning and expression analysis of cinnamoyl-CoA reductase (CCR) genes in sorghum. *PeerJ* **2016**, *4*, e2005. [[CrossRef](#)] [[PubMed](#)]
56. Ye, J.; Coulouris, G.; Zaretskaya, I.; Cutcutache, I.; Rozen, S.; Madden, T.L. Primer-BLAST: A tool to design target-specific primers for polymerase chain reaction. *BMC Bioinform.* **2012**, *13*, 134. [[CrossRef](#)] [[PubMed](#)]
57. Jin, Y.; Liu, F.; Huang, W.; Sun, Q.; Huang, X. Identification of reliable reference genes for qRT-PCR in the ephemeral plant *Arabidopsis pumila* based on full-length transcriptome data. *Sci. Rep.* **2019**, *9*, 8408. [[CrossRef](#)] [[PubMed](#)]
58. Livak, K.J.; Schmittgen, T.D. Analysis of relative gene expression data using real-time quantitative PCR and the $2^{-\Delta\Delta CT}$ method. *Methods* **2001**, *25*, 402–408. [[CrossRef](#)] [[PubMed](#)]
59. Motulsky, H. Prism 5 statistics guide, 2007. *GraphPad Softw.* **2007**, *31*, 39–42.
60. Ward, D.M.; Vaughn, M.B.; Shiflett, S.L.; White, P.L.; Pollock, A.L.; Hill, J.; Schnegelberger, R.; Sundquist, W.I.; Kaplan, J. The role of LIP5 and CHMP5 in multivesicular body formation and HIV-1 budding in mammalian cells. *J. Biol. Chem.* **2005**, *280*, 10548–10555. [[CrossRef](#)] [[PubMed](#)]
61. Hu, X.; Yang, P.; Chai, C.; Liu, J.; Sun, H.; Wu, Y.; Zhang, M.; Zhang, M.; Liu, X.; Yu, H. Structural and mechanistic insights into fungal β -1, 3-glucan synthase FKS1. *Nature* **2023**, *616*, 190–198. [[CrossRef](#)] [[PubMed](#)]
62. Yu, J.; Wang, J.; Lin, W.; Li, S.; Li, H.; Zhou, J.; Ni, P.; Dong, W.; Hu, S.; Zeng, C. The genomes of *Oryza sativa*: A history of duplications. *PLoS Biol.* **2005**, *3*, e38. [[CrossRef](#)]
63. Venkateswaran, K.; Elangovan, M.; Sivaraj, N. Origin, domestication and diffusion of *Sorghum bicolor*. In *Breeding Sorghum for Diverse end Uses*; Elsevier: Amsterdam, The Netherlands, 2019; pp. 15–31.
64. Shen, Y.; Liu, M.; Wang, L.; Li, Z.; Taylor, D.C.; Li, Z.; Zhang, M. Identification, duplication, evolution and expression analyses of caleosins in Brassica plants and *Arabidopsis* subspecies. *Mol. Genet. Genom.* **2016**, *291*, 971–988. [[CrossRef](#)]
65. Niu, Q.; Zhang, P.; Su, S.; Jiang, B.; Liu, X.; Li, C.; Yu, T.; Yi, H.; Tang, J.; Cao, M. Characterization and expression analyses of Callose synthase enzyme (Cals) family genes in maize (*Zea mays* L.). *Biochem. Genet.* **2022**, *60*, 351–369. [[CrossRef](#)] [[PubMed](#)]
66. Wang, Y.; Li, X.; Fan, B.; Zhu, C.; Chen, Z. Regulation and function of defense-related callose deposition in plants. *Int. J. Mol. Sci.* **2021**, *22*, 2393. [[CrossRef](#)]
67. Shikanai, Y.; Yoshida, R.; Hirano, T.; Enomoto, Y.; Li, B.; Asada, M.; Yamagami, M.; Yamaguchi, K.; Shigenobu, S.; Tabata, R. Callose synthesis suppresses cell death induced by low-calcium conditions in leaves. *Plant Physiol.* **2020**, *182*, 2199–2212. [[CrossRef](#)] [[PubMed](#)]
68. Kauss, H.; Jeblick, W. Induced Ca^{2+} uptake and callose synthesis in suspension-cultured cells of *Catharanthus roseus* are decreased by the protein phosphatase inhibitor okadaic acid. *Physiol. Plant.* **1991**, *81*, 309–312. [[CrossRef](#)]
69. Verma, D.P.S.; Hong, Z. Plant callose synthase complexes. *Plant Mol. Biol.* **2001**, *47*, 693–701. [[CrossRef](#)] [[PubMed](#)]
70. He, D.; You, X.-L.; He, S.-L.; Zhang, M.-X.; Zhang, J.-R.; Hua, C.; Wang, Z.; Liu, Y.-P. Identification of callose synthetase gene family and functional analysis of P1CalS5 in *Paeonia lactiflora*. *Sci. Agric. Sin.* **2023**, *56*, 3183–3198.
71. Dong, X.; Hong, Z.; Sivaramakrishnan, M.; Mahfouz, M.; Verma, D.P.S. Callose synthase (CalS5) is required for exine formation during microgametogenesis and for pollen viability in *Arabidopsis*. *Plant J.* **2005**, *42*, 315–328. [[CrossRef](#)] [[PubMed](#)]
72. Enns, L.C.; Kanaoka, M.M.; Torii, K.U.; Comai, L.; Okada, K.; Cleland, R.E. Two callose synthases, GSL1 and GSL5, play an essential and redundant role in plant and pollen development and in fertility. *Plant Mol. Biol.* **2005**, *58*, 333–349. [[CrossRef](#)] [[PubMed](#)]
73. Ren, L.; Tang, D.; Zhao, T.; Zhang, F.; Liu, C.; Xue, Z.; Shi, W.; Du, G.; Shen, Y.; Li, Y. Os SPL regulates meiotic fate acquisition in rice. *New Phytol.* **2018**, *218*, 789–803. [[CrossRef](#)]
74. Zhang, Z.; Lee, Y.; Spetz, C.; Clarke, J.L.; Wang, Q.; Blystad, D.-R. Invasion of shoot apical meristems by *Chrysanthemum stunt viroid* differs among *Argyranthemum* cultivars. *Front. Plant Sci.* **2014**, *6*, 53. [[CrossRef](#)]
75. Liu, F.; Zou, Z.; Fernando, W.D. Characterization of callose deposition and analysis of the callose synthase gene family of brassica napus in response to leptosphaeria maculans. *Int. J. Mol. Sci.* **2018**, *19*, 3769. [[CrossRef](#)]

76. Huang, Q.; Lin, B.; Cao, Y.; Zhang, Y.; Song, H.; Huang, C.; Sun, T.; Long, C.; Liao, J.; Zhuo, K. CRISPR/Cas9-mediated mutagenesis of the susceptibility gene OsHPP04 in rice confers enhanced resistance to rice root-knot nematode. *Front. Plant Sci.* **2023**, *14*, 1134653. [[CrossRef](#)]
77. Sun, M.; Voorrips, R.E.; Steenhuis-Broers, G.; van't Westende, W.; Vosman, B. Reduced phloem uptake of *Myzus persicae* on an aphid resistant pepper accession. *BMC Plant Biol.* **2018**, *18*, 138. [[CrossRef](#)] [[PubMed](#)]
78. Han, X.; Hyun, T.K.; Zhang, M.; Kumar, R.; Koh, E.-j.; Kang, B.-H.; Lucas, W.J.; Kim, J.-Y. Auxin-callose-mediated plasmodesmal gating is essential for tropic auxin gradient formation and signaling. *Dev. Cell* **2014**, *28*, 132–146. [[CrossRef](#)] [[PubMed](#)]
79. Liu, J.; Du, H.; Ding, X.; Zhou, Y.; Xie, P.; Wu, J. Mechanisms of callose deposition in rice regulated by exogenous abscisic acid and its involvement in rice resistance to *Nilaparvata lugens* Stål (Hemiptera: Delphacidae). *Pest Manag. Sci.* **2017**, *73*, 2559–2568. [[CrossRef](#)]
80. Wang, B.; Andargie, M.; Fang, R. The function and biosynthesis of callose in high plants. *Heliyon* **2022**, *8*, e09248. [[CrossRef](#)]
81. Zhu-Salzman, K.; Salzman, R.A.; Ahn, J.-E.; Koiwa, H. Transcriptional regulation of sorghum defense determinants against a phloem-feeding aphid. *Plant Physiol.* **2004**, *134*, 420–431. [[CrossRef](#)]
82. Fan, J.; Zhang, X.-Y.; Sun, X.-Z.; Xu, B.-Y. Effect of methyl jasmonate on aphid resistance of chrysanthemum. *Ying Yong Sheng tai xue bao J. Appl. Ecol.* **2020**, *31*, 4197–4205.
83. Underwood, W. The plant cell wall: A dynamic barrier against pathogen invasion. *Front. Plant Sci.* **2012**, *3*, 85. [[CrossRef](#)]
84. Repka, V.; Fischerova, I.; Šilhárová, K. Methyl jasmonate is a potent elicitor of multiple defense responses in grapevine leaves and cell-suspension cultures. *Biol. Plant.* **2004**, *48*, 273–283. [[CrossRef](#)]
85. Yao, L.; Guo, X.; Su, J.; Zhang, Q.; Lian, M.; Xue, H.; Li, Q.; He, Y.; Zou, X.; Song, Z. ABA-CsABI5-CsCalS11 module upregulates Callose deposition of citrus infected with *Candidatus Liberibacter asiaticus*. *Hortic. Res.* **2024**, *11*, uhad276. [[CrossRef](#)] [[PubMed](#)]
86. Ton, J.; Flors, V.; Mauch-Mani, B. The multifaceted role of ABA in disease resistance. *Trends Plant Sci.* **2009**, *14*, 310–317. [[CrossRef](#)] [[PubMed](#)]
87. Wu, J.; Wang, L.; Baldwin, I.T. Methyl jasmonate-elicited herbivore resistance: Does MeJA function as a signal without being hydrolyzed to JA? *Planta* **2008**, *227*, 1161–1168. [[CrossRef](#)] [[PubMed](#)]
88. Snoeck, S.; Guayazán-Palacios, N.; Steinbrenner, A.D. Molecular tug-of-war: Plant immune recognition of herbivory. *Plant Cell* **2022**, *34*, 1497–1513. [[CrossRef](#)] [[PubMed](#)]
89. Farmer, E.E.; Gao, Y.Q.; Lenzoni, G.; Wolfender, J.L.; Wu, Q. Wound-and mechanostimulated electrical signals control hormone responses. *New Phytol.* **2020**, *227*, 1037–1050. [[CrossRef](#)]
90. Wang, F.; Zhao, S.; Han, Y.; Shao, Y.; Dong, Z.; Gao, Y.; Zhang, K.; Liu, X.; Li, D.; Chang, J. Efficient and fine mapping of RMES1 conferring resistance to sorghum aphid *Melanaphis sacchari*. *Mol. Breed.* **2013**, *31*, 777–784. [[CrossRef](#)]
91. Puri, H. *Sorghum-Sugarcane Aphid Interactions: Multi-Omic Approaches to Elucidate Plant Defense Against Sap-Feeding Insects*; The University of Nebraska-Lincoln: Lincoln, NE, USA, 2023.

Disclaimer/Publisher's Note: The statements, opinions and data contained in all publications are solely those of the individual author(s) and contributor(s) and not of MDPI and/or the editor(s). MDPI and/or the editor(s) disclaim responsibility for any injury to people or property resulting from any ideas, methods, instructions or products referred to in the content.